

## Preparation And Structural Properties Of Aluminium Substituted Lithium Nano Ferrites By Citrate-Gel Auto Combustion Method

G. Aravind, D. Ravinder

Department of physics, Nizam College,Osmania University, Hyderabad-500001

### Abstract:

Nano sized particles of aluminium doped lithium nano ferrites having general formula  $\text{Li}_{0.5} \text{Al}_x \text{Fe}_{2.5-x} \text{O}_4$  (where  $x=0.0,0.2,0.4,0.6,0.8,1.0$ ) were prepared by the citrate gel method at low temperature ( $180^\circ\text{C}$ ). The synthesized powders were sintered at  $500^\circ\text{C}$  for 4 hours. The crystal structure characterization of the sintered powders were carried out by using X-ray diffraction(XRD). The X-Ray diffraction analysis confirmed the formation of single phase cubic spinel structure. The average particle size of the synthesized powders was 13 to 27nm. The surface morphology were studied by Scanning Electron Microscopy (SEM) which revealed the formation of largely agglomerated nano particles. Lattice parameter, X-ray density, experimental density, porosity of the samples were calculated. The observed results can be discussed in this paper on the basis of composition.

### I. Introduction:

The study of nanoferrites has attracted immense attention of the scientific community because of their novel properties and technological applications especially when the size of the particle approaches to the nanometer scale. More novel electrical and magnetic behavior have been observed in comparison with their bulk counterpart.[1-2]. In general, the transport properties of the nano materials are predominantly controlled by the grain boundaries than by the grain itself[3]. Due to this reason, the magnetic materials have explored a wide range of applications and thus are replacing conventional methods.

Commonly used ferrites are primarily classified into three types: spinels, hexagonal ferrites, and garnets according to their primary crystal lattice. Generally, ferrimagnetism arises from the antiparallel alignment of the magnetic moments on transition metal ions, present on different magnetic sublattices. The origin of the antiparallel coupling can be explained by super-exchange of valence electrons between the filled p-orbitals of  $\text{O}^{2-}$  and unfilled d-orbitals of the transition metal cations.

Spinel ferrites have the general formula  $\text{MO.Fe}_2\text{O}_3$  where M represents a divalent transition ion or a combination of ions having an average valence of two. The crystal structure of a ferrite can be regarded as an interlocking network of positively charged metal ions and negatively charged divalent oxygen ions. In spinel ferrites, the relatively large oxygen anions form a cubic close packing with  $\frac{1}{2}$  of the octahedral and  $\frac{1}{8}$  of the tetrahedral interstitial sites occupied by metal ions.

Lithium ferrite has been a widely investigated material due to its impotence in construction and engineering of many electromagnetic and microwave devices[4-6].Bulk lithium ferrite has an inverse cation distribution of the form  $(\text{Fe}^{3+})_A[\text{Li}_{0.5} \text{Fe}_{1.5}]_B$ . The interplay between the superexchange interactions of  $\text{Fe}^{3+}$  ions at A and B sublattices gives rise to ferri magnetic ordering of magnetic moments[7,8].Ease of fabrication, low cost, high Curie temperature and better temperature stability of saturation magnetization of lithium ferrites have made them attractive from commercial point of view and are good substitutes of garnets for microwave devices such as isolators, circulators, gyrators, and phase shifters. Lithium ferrite has an important role in microwave latching devices, magnetic switching circuits and can also be used as cathode material in lithium batteries. There are many reports on the effect of magnetic and non-magnetic substitutions on various properties of lithium ferrite[9-12].

Nano ferrites were usually prepared by the conventional ceramic methods but the resultant products are not necessarily always stoichiometric or homogeneous[13]. A variety of chemical synthesis methods such as co-precipitation, hydrothermal synthesis, and sol-gel process have been developed.[14-16]. The Citrate-gel auto combustion technique has been used for the preparation of mixed nano crystalline spinel ferrites with specific properties, such as controlled stoichiometry and narrow particle size distribution. The low cost, simplicity and short time of production and the purity and homogeneity of final product are included among its advantages[17].

## II. Experimental Details:

The Aluminium substituted lithium nano ferrite particles having the general formula  $\text{Li}_{0.5}\text{Al}_x\text{Fe}_{2.5-x}\text{O}_4$  (where  $x=0.0,0.2,0.4,0.6,0.8,1.0$ ) were synthesized by citrate-gel auto combustion technique at a very low temperature (180°C) using the below mentioned raw materials.

### 2.1 Raw Materials:

- \*Lithium Nitrate-99% Pure (AR Grade) ( $\text{LiNO}_3$ )
- \*Aluminum Nitrate-99% Pure (AR Grade) ( $\text{Al}(\text{NO}_3)_3 \cdot 9\text{H}_2\text{O}$ )
- \*Ferric Nitrate-99% pure (AR grade) ( $\text{Fe}(\text{NO}_3)_3 \cdot 9\text{H}_2\text{O}$ )
- \*Citric acid - 99% pure (AR grade) ( $\text{C}_6\text{H}_8\text{O}_7 \cdot \text{H}_2\text{O}$ )
- \*Ammonia - 99% pure (AR grade) ( $\text{NH}_3$ )

### 2.2. Synthesis:

Required quantities of metal nitrates were dissolved in a minimum quantity of distilled water and mixed together. Aqueous solution of Citric acid was then added to the mixed metal nitrate solution. Ammonia solution was then added with constant stirring to maintain  $\text{pH}$  of the solution at 7. The resulting solution was continuously heated on the hot plate at

100°C up to dryness with continuous stirring. A viscous gel has resulted. Increasing the temperature up to 200°C lead the ignition of gel. The dried gel burnt completely in a self propagating combustion manner to form a loose powder. The burnt powder was ground in Agate Mortar and Pestle to get a fine ferrite powder. Finally the burnt powder was calcinated in air at 500°C temperature for four hours and cooled to room temperature.

**2.3. XRD Analysis:** Structural characterization of the prepared samples were carried out using X-ray Diffraction with  $\text{Cu } k_\alpha$  radiation of wavelength 1.5405 Å. Using these we study the single phase nature and nano-phase formation of the Li-Al ferrite system at room temperature by continuous scanning in the range of 10° to 80° in steps of 0.04°/Sec.

The crystalline size was calculated for all the samples using the high intensity peak and using the Debye Scherrer formula [18] while taking into account the intensity broadening [19]. The Debye Scherrer formula assumes approximations and gives the average grain size if the grain size distribution is narrow and strain induced effects are small.

Scherrer Formula:

$$\text{Crystalline size of the sample } D = \frac{0.91\lambda}{\beta \cos\theta}$$

- Where  $\lambda$  is the wavelength of X-ray used [20]
- $\beta$  is the Width of diffraction peak i.e. Full Width Half Maxima (FWHM) in radians.
- $\theta$  is the peak position.

Lattice parameter (a) of the sample was calculated by the formula

$$a = d * \sqrt{h^2 + k^2 + l^2} \quad [20]$$

- Where a= Lattice Constant
- (hkl) are the Miller Indices
- d is the inter planner spacing,

The X-ray density of the prepared sample was calculated using the relation

$$d_X = \frac{nM}{a^3 N} \text{ [g/cm}^3\text{]} \quad [21]$$

- Where M = molecular weight of the sample
- n is the number of molecules in a unit cell of spinel lattice.
- a is the lattice parameter and N is the Avogadro number.

The Volume of the Unit Cell  $V = a^3$

The experimental density of the prepared sample was calculated by Archimedes's principle with xylene media using following relation.

$$d_E = \frac{\text{Weight of the sample in air}}{\text{Weight of the sample in air} - \text{Weight of the sample in xylene}} \times \text{Density of Xylene}$$

The Percentage of Porosity P of the ferrite sample was then determined by employing the relation

$$P = \frac{d_X - d_E}{d_X} \times 100$$

Where  $d_X$  is the X-ray density &  $d_E$  is the experimental density. The distance between the magnetic ions (hoping length) on A-site (Tetrahedral) and B site (Octahedral) is calculated according to the following relations

$$d_A = 0.25a\sqrt{3} \quad \text{and} \quad d_B = 0.25a\sqrt{2} \quad [22]$$

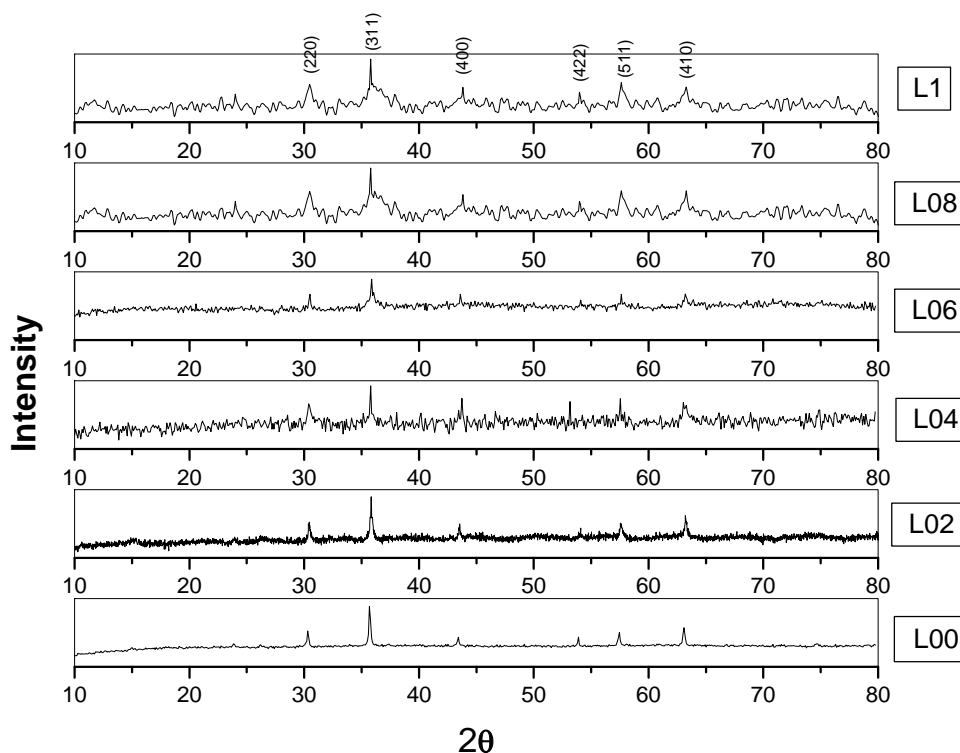
Where 'a' is the lattice parameter

### 2.4SEM Studies:

Micro structural analysis (surface morphology) of the prepared samples was carried out by scanning Electron microscopy (SEM).

### III. Results and Discussions:

The X-ray diffraction pattern of the Aluminum substituted lithium nano ferrites were shown in fig(1). It can be seen from the figure all Bragg's reflections have been indexed, which confirm the formation of cubic spinel structure in single phase without any impurity peak. The strongest reflection comes from the (311) plane, which denotes the spinel phase. The peaks indexed to (220)(311)(400)(422)(511) and (410) of a cubic uni cell, all planes are the allowed planes which indicates the formation of cubic spinel structure in single phase.



**Fig(1): XRD Pattern of Li-Al Nano ferrites**

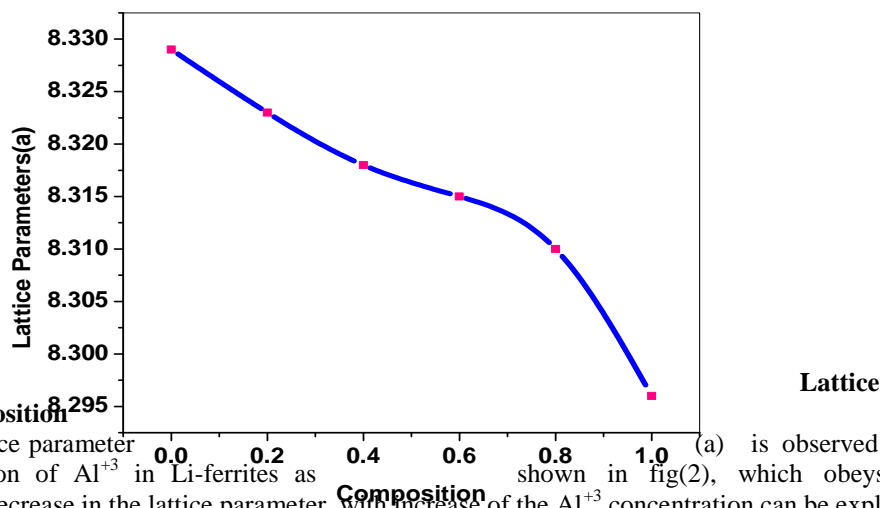
The calculated values of crystalline size for the different compositions are given in the table(1).

It can be seen from the table that the values of the crystal size varies from 13nm to 27nm. The crystalline size was not same for all Al concentrations because the preparation condition followed here which gave rise to different rate of ferrite formation for different concentrations of Al, favoring the variation of crystalline size. Conventional methods needs to high temperatures and more time, but in this method, ferrite phase can be produced very fast at low temperature.

**Table (1). Values of the Crystalline size, Lattice parameter(a), X-ray density( $d_x$ ), Experimental density( $d_p$ ) and Porosity.**

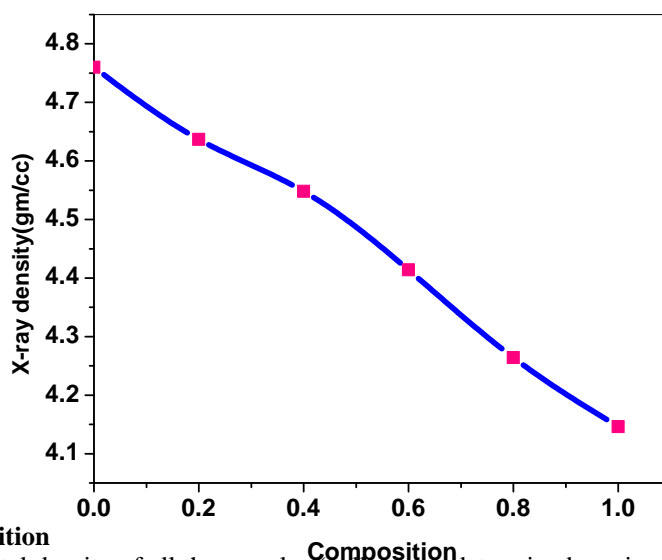
| Sl. No | Composition  | Molecular weight | Particle size(D) nm | Lattice parameter A° | X-ray Density gm/cc | Expt Density gm/cc | Porosity (%) |
|--------|--|------------------|---------------------|----------------------|---------------------|--------------------|--------------|
| 1      | Li <sub>0.5</sub> Fe <sub>2.5</sub> O <sub>4</sub>                   | 207.091          | 27.31               | 8.329                | 4.760               | 4.388              | 7.8          |
| 2      | Li <sub>0.5</sub> Al <sub>0.2</sub> Fe <sub>2.3</sub> O <sub>4</sub> | 201.317          | 24.82               | 8.323                | 4.637               | 4.206              | 9.2          |
| 3      | Li <sub>0.5</sub> Al <sub>0.4</sub> Fe <sub>2.1</sub> O <sub>4</sub> | 195.543          | 17.69               | 8.318                | 4.548               | 4.138              | 9.0          |
| 4      | Li <sub>0.5</sub> Al <sub>0.6</sub> Fe <sub>1.9</sub> O <sub>4</sub> | 189.770          | 18.71               | 8.315                | 4.414               | 4.074              | 7.7          |
| 5      | Li <sub>0.5</sub> Al <sub>0.8</sub> Fe <sub>1.7</sub> O <sub>4</sub> | 183.996          | 15.98               | 8.310                | 4.264               | 3.976              | 6.7          |
| 6      | Li <sub>0.5</sub> Al <sub>1.0</sub> Fe <sub>1.5</sub> O <sub>4</sub> | 178.223          | 13.74               | 8.296                | 4.146               | 3.835              | 7.5          |

The lattice parameter values of all the compositions of aluminum doped lithium nano ferrites have been calculated from the d-spacing and are given in the above table. A plot is drawn between the lattice parameter vs Aluminum ionic content (composition) is shown in fig (2).



**Fig(2):Variation of Parameter vs Composition**

The decrease in the lattice parameter with increase in concentration of  $Al^{+3}$  in Li-ferrites as shown in fig(2), which obeys the Vegard;s law[23]. The decrease in the lattice parameter with increase of the  $Al^{+3}$  concentration can be explained on the basis of the relative ionic radii of the  $Al^{+3}$  and  $Fe^{+3}$  ions since radius of  $Al^{+3}$  ( $0.535A^{\circ}$ ) is smaller than that of  $Fe^{+3}$  ( $0.645A^{\circ}$ )[24]. The substitution of smaller ions by larger ions results in the shrinkage of the lattice[25]. The decrease in the value of the lattice parameter when Fe is replaced by the Al, as observed in the present work, is therefore expected.



**Fig(3):Variation of**

**X-ray density with composition**

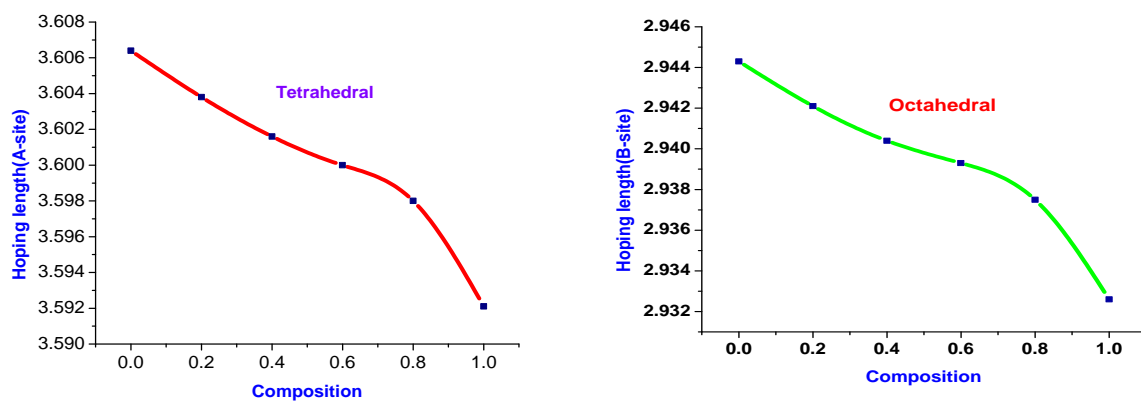
The values of the experimental density of all the samples (pellets) are determine by using Archimedes principle are given in table (1). From the table it can be observed that experimental density of the Al substituted Li ferrites was observed to be decrease with Al concentration, while all the other experimental conditions were kept identical for these samples[26]. Enhanced densification of the samples are observed in the citrate gel prepared samples, this is the one of the advantage of this preparation technique. The experimental density values are observed to be >85% of the densities evaluated from X-ray diffraction. The values are found to be in the range 3.835 to 4.388 gm/cc for Aluminum doped Lithium ferrites.

A graph is plot between the X-ray density ( $d_x$ ) vs Al concentration is shown in fig(3). From the graph one can be observed that experimental density of the Al substituted Li ferrites was observed to be decrease with Al concentration. The X-ray density ( $d_x$ ) is depend on the lattice parameter and molecular weight of the sample. From the table one can observe that molecular weight of the sample is decreases with Aluminum concentration and lattice parameter is also decreased. This may due to the greater atomic weight of Fe-55.85gm/mol and lesser atomic weight of Al-26.98gm/mol. [27]

**Table(2): Values of the Volume(V), Hopping length of A-site and B-site:**

| S.No | Composition   | Volume( $\text{\AA}^3$ ) | A-site( $d_A$ ) | B-site( $d_B$ ) |
|------|---|--------------------------|-----------------|-----------------|
| 1    | $\text{Li}_{0.5}\text{Fe}_{2.5}\text{O}_4$                | 577.801                  | 3.6064          | 2.9443          |
| 2    | $\text{Li}_{0.5}\text{Al}_{0.2}\text{Fe}_{2.3}\text{O}_4$ | 576.553                  | 3.6038          | 2.9421          |
| 3    | $\text{Li}_{0.5}\text{Al}_{0.4}\text{Fe}_{2.1}\text{O}_4$ | 575.515                  | 3.6016          | 2.9404          |
| 4    | $\text{Li}_{0.5}\text{Al}_{0.6}\text{Fe}_{1.9}\text{O}_4$ | 574.892                  | 3.6000          | 2.9393          |
| 5    | $\text{Li}_{0.5}\text{Al}_{0.8}\text{Fe}_{1.7}\text{O}_4$ | 573.856                  | 3.5980          | 2.9375          |
| 6    | $\text{Li}_{0.5}\text{Al}_{1.0}\text{Fe}_{1.5}\text{O}_4$ | 570.960                  | 3.5921          | 2.9326          |

The calculated values of the Volume of the unit cell are tabulated in table(2). The Volume of the unit cell is depend upon the lattice parameter. In the present case, the volume of unit cell of the Li-Al system is decreases with increase of the Al concentration because lattice parameter is decreases with increase of Al concentration.



**Fig(4): Variation of Hopping Length with Composition**

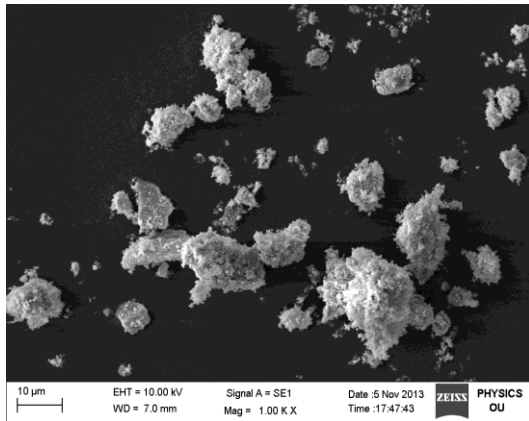
The values of the hopping length of the tetrahedral site( $d_A$ ) and Octahedral site ( $d_B$ ) are calculated and tabulated in the table (2). A plot is drawn between the hopping length of the tetrahedral site( $d_A$ ) and Octahedral site( $d_B$ ) as a function of Aluminum concentration is shown in fig(4).

It is observed that the distance between the magnetic ions decreases with the increase of the Al content, because ionic radius of  $\text{Al}^{+3}$  ( $53\text{\AA}^0$ ) is smaller than the  $\text{Fe}^{+3}$  ( $64\text{\AA}^0$ ), which makes the magnetic ions closer to each other and hopping length decreases.

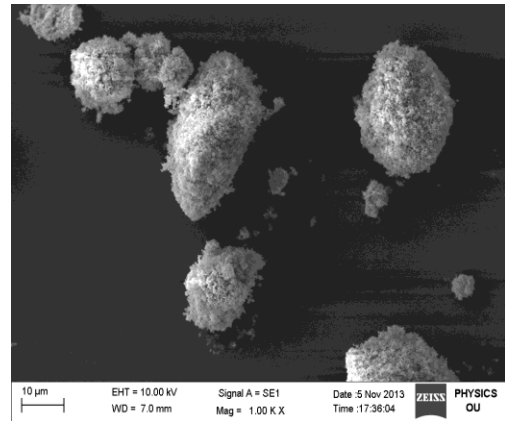
**Surface Morphology by SEM:**

The surface morphology of the sintered samples were studied using SEM(Scanning Electron Microscope). The secondary electron images are taken at different magnifications to study the morphology of samples by SEM. Fig(5) shows the SEM micro structures of the Aluminum doped Lithium nano ferrites.

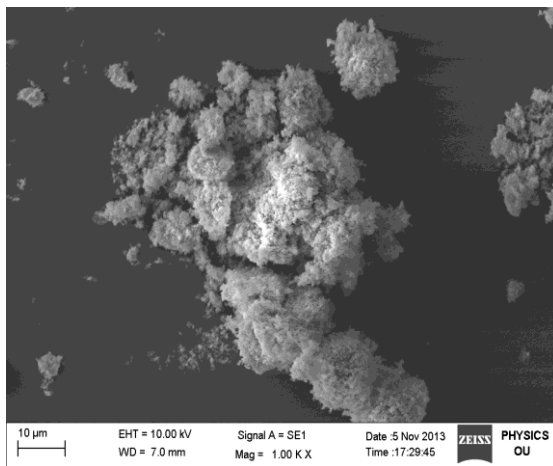
The morphology and grain size of the samples seem to be non uniform with somewhat agglomeration in the synthesized samples which is unavoidable. From the preliminary observations of the SEM images, one can observe that the grain size is slightly affected by the Al doping concentration.



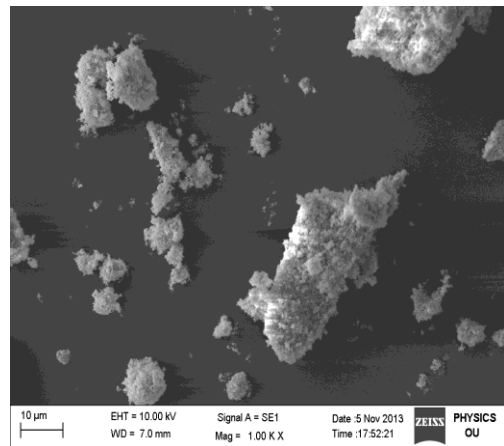
x=0.0



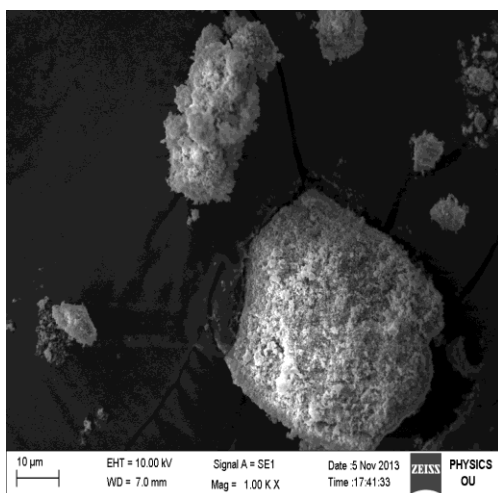
x=0.2



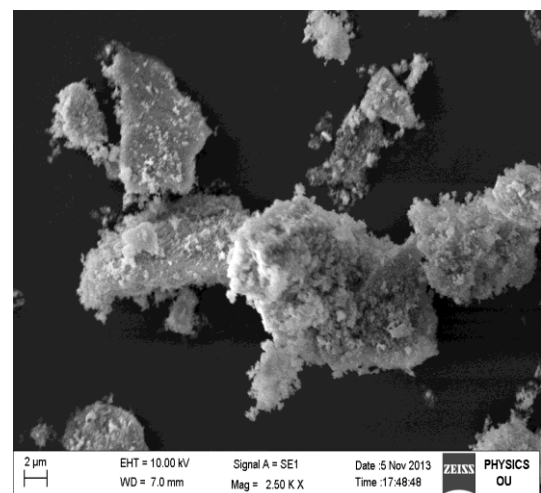
x=0.4



x=0.6



x=0.8



x=1.0

**Fig(5). SEM micrographs of compositions of Li-Al Nano Ferrites**

#### IV. Conclusoins:

- The Citrate-Gel auto combustion method to be a convenient method for obtaining homogeneous mixed Li-Al nano ferrites without any impurity peak and material loss.
- X-ray diffraction pattern confirm that the formation of single phase cubic spinel structure. The crystalline size of the nano ferrites in the range 13-27nm.
- The lattice parameter is decreases with increase of Al composition in Li nano ferrites indicate that the mixed Li-Al nano ferrites obey Vegard's law.
- The distance between the magnetic ions on A and B calculated. It is clear that the distance between the magnetic ions decreases with increasing the Al content.
- SEM analysis explain that the morphology of the particle is similar and particle sharpness is more or less spherical with some cluster/agglomeration between the particles.

#### V. Acknowledgements:

The authors are very grateful to Prof.K.Venugopal Reddy, Head, Department of Physics, College of Science, Osmania University, Hyderabad. And Prof.T.L.N.Swamy, Principal, Nizam College, Basheerbagh,Hyderabad for their encouragement in research work. The authors are also thankful to UGC, New Delhi, for the award of UGC major research project.

#### REFERNCES

- [1]. Subhash C, Srivatsava BK, Anjali K, Magnetic behavior of nano-particles of  $Ni_{0.5}Co_{0.5}Fe_2O_4$  prepared using two different routes, Indian Journal of Pure App Phy.2004;42:366-367.
- [2] Kittle C.Domain theory and the dependence of the coercive force of fine ferromagnetic fine powders on particle size. Phy, Rev,1948;73:810-811 doi:10.1103/PhysRev73.810
- [3]. Kale A, Gubbala S,Misara RDK, Magnetic behavior of nano crystalline nickel ferrite synthesized by the reverse micelle technique. J Magn Magn Mater 2004;3:350-358.
- [4] Baba, p.D.; Argentina, G.M.; Courtney, W.E.;Dionne, G.F.;Temme, T.H.Fabrication and properties of microwave lithium ferrites.IEEE Transactions on Magnetics.1972,MAG-8,83-94
- [5] George M.; Nair, S,S; John A.M; Joy, P.A.;Anantharaman, M.R. Structural magnetic and electrical properties of the sol-gel prepared lithium

- fineparticlesJ.Phys.D;Appl.Phys2006,39,90 0- 910.
- [6] Dionne, G.F. Properties of ferrites at low temperatures (invited). J.Appl.Phy., 1997,81,5064-5069.
- [7] Hessien M.M Synthesis and characterization of lithium ferrite by oxalate precursor route J.Magn.Magn.Mater., 2008 320,2800-2807.
- [8] Fu, Y-P; Lin,C-H.;Liu,C.-W.; Yao,Y-D. Microwave induced combustion synthesis of  $Li_{0.5}Fe_{2.5}O_4$  powder and their characterization. J.Alloys Comp.,2005, 395,247-251
- [9] B.K.Kumar, Effect of the strong relaxor cobalt on the parallel and perpendicular pumping spin wave instability threshold of LiTi ferrites, J.Magn,Mag.,Mater 163 (1996)164.
- [10] S.C.Watawe, B.D. Sarwade, S.S.Bellad, B.D.Sutar, B.K,Chougule Micro-structure, frequency and temperature dependent dielectric properties of Cobalt substituted lithium ferrites j.Magn.Magn.Mater 214(1-2)2000, 55
- [11] Y.C.Venudhar, K.S. Mohan, Dielectric behavior of lithium-ccobalt mixed ferrites, mater.Letter 54(2002)135.
- [12] S.A.Jadhav, Magnetic properties of Zn substituted Li-Cu ferrites, J.Magn.Magn.Mater.224(2001)167
- [13] A.Verma, T.Goel, R.Mendiratta, P.Kishan , J.Magn.Magn.Mater 208(2000) 19.
- [14] V.V.Pankov, M.Pernet, P.Germi, P. Mollard,j.Magn.Magn,mater 120(1993)69.
- [15] P.S.A.Kumar, J.J. Shrotri C.E. Deshpande, J.Appl.Phys 81(1997)4788.
- [16] A.Dias, R.L.Moreria, N.D.S.Mohallen, J. J.Magn Magn Mater172(1997)L9
- [17] K.RamaKrishna, K.Vijay Kumar, C.Ravinderguptha, Dachehalli Ravinder, Advances in Materials Physics and Chemistry,2012,2,149-154
- [18] Cullity B D, Elements of X-ray Diffraction (Addition Wesely<Reading mass), 1959,p132.
- [19] Mahmud ST, Akther Hossain AKM, Abdul Hakim AKM, Seki M,KawaiT, Tabata H(2006)J Magn Magn mater 305: 269 doi:10.1016/j.jmmm.2006.01.012
- [20] B.P.Ladgaonkar, P.P.Bakare,S.R. Sainkar and A.S.Vaingankar, "Influence of  $Nd^{+3}$  substitution on permeability spectrum of Zn-Mg ferrite". Materials Chemistry and Physics, Volume 69,Issues 1- 3, March 1, 2001, pages 19-24.
- [21] R.C. Kumbale.P.A.Shaik,S.S.Kamble, Y.D.Kolekar, J.Alloys Compound, 478 (2009) p.599 doi:10.1016/j.jmmm.2005.03.007

- [22] B.Vishvanathan, V.R.K.Murthy, Ferrite Materials Science and Technology, Narosa Public House, New Delhi (1990)
- [23] L.Vergard, Z. Phys, 5 (1921) 17, [doi:10.1007/BF01349680](https://doi.org/10.1007/BF01349680)
- [24] M.Abdullah Dar, Khalid Mujasam Batoo, Vivek verma, Journal of Alloys and Compounds, Vol-493, issue 1-2, 18 march, 2010, pages 553-560
- [25] M.Raghasudha, D.Ravinder, Veerasomaiah, Advanced Materials letters [doi:10.5185/amlett.2013.5479](https://doi.org/10.5185/amlett.2013.5479)
- [26] M.P.Pandya, K.B.Modi, H.H.Josshi, Journal of Materials Science 40 (2005) , 5223-5232.
- [27] K.B.Modi, J.D.Gajera, M.P.Pandya, H.G.Vora, H.H.Joshi, Pramana Journal of Physics, Vol 62, No 5, May, 2004, pages 1173-1180.